



HAL
open science

The linear PT-Symmetric complex potential

R. Lombard, R. Mezhoud

► **To cite this version:**

R. Lombard, R. Mezhoud. The linear PT-Symmetric complex potential. Romanian Journal of Physics, 2017, 62, pp.112. in2p3-01997748

HAL Id: in2p3-01997748

<https://hal.in2p3.fr/in2p3-01997748>

Submitted on 29 Jan 2019

HAL is a multi-disciplinary open access archive for the deposit and dissemination of scientific research documents, whether they are published or not. The documents may come from teaching and research institutions in France or abroad, or from public or private research centers.

L'archive ouverte pluridisciplinaire **HAL**, est destinée au dépôt et à la diffusion de documents scientifiques de niveau recherche, publiés ou non, émanant des établissements d'enseignement et de recherche français ou étrangers, des laboratoires publics ou privés.

THE LINEAR PT-SYMMETRIC COMPLEX POTENTIAL

R. J. LOMBARD¹, R. MEZHOUD²

¹Groupe de Physique Théorique, Institut de Physique Nucléaire, 91406 Orsay Cedex, France

²Faculté des Sciences, Université de Boumerdes, Algeria

Received December 14, 2016

Abstract. The spectrum of a PT-symmetric complex-valued linear potential is investigated. Working in the $D = 1$ dimensional space, we consider $\mathcal{V}(x) = \lambda|x| + icx$. Semianalytical solutions are given by using the properties of the Airy functions. The numerical integration of the differential equation system is discussed. We show that the number of eigenstates with a real eigenvalue is limited, depending on the ratio c/λ and on the quantum number n . This is reflecting the spontaneous breaking of PT symmetry. For the ground state, we conjecture the eigenvalue to be real for any value of c .

Key words: Quantum mechanics; bound states; complex PT-symmetric potentials.

PACS: 03.65.Ge; 03.65-w; 03.65.Fd.

1. INTRODUCTION

The discovery of PT-symmetric complex-valued potentials, with real eigenvalues, has generated a large amount of research papers; see, for example, Refs. [1, 2] and previous papers quoted in these articles. Numerous examples of spectra have been calculated, some of them analytically. In general, these external potentials belong to the class of real-valued potentials admitting analytical solutions. The archetype is the harmonic oscillator given by Znojil [3]. Other relevant examples have been also reported [4–10].

In the last 10-15 years, the domain of nonhermitian Hamiltonians has witnessed many developments. Perhaps the most promising one is the extension of the canonical quantum mechanics. It is enlarging the class of physical problems to be handled *via* the Schrödinger equation [11]. Consequently, many aspects of quantum physics have been revisited introducing PT-symmetric potentials. It concerns soliton formation and light propagation in optical media, Bloch oscillations, and other physical realizations. For instance, the PT-symmetric potential scattering in a planar slab waveguide has been studied [12]. Recent papers give further interesting applications in relevant physical situations for both linear and nonlinear PT-symmetric systems [13–17]. The few published review articles give comprehensive overviews of this fast growing research area [18–20].

The present paper addresses a very specific problem. To the best of our knowledge, the linear potential case has been only partially investigated. A variational

ansatz have been used by Bender *et al.* [21] to study $\mathcal{V}(x) = (ix)^N$. The purpose of the present work is to discuss the spectrum of the linear complex-valued potential

$$\mathcal{V}(x) = \lambda|x| + icx. \quad (1)$$

At first glance, the problem sounds trivial. However, it has some surprising effects.

The paper is organized as follows. Section 2 is devoted to semianalytical solutions, based on the Airy functions. By using a simple parametrization of the Airy function, the qualitative aspects of the results are illustrated in Sec. 3 for the ground and first excited states. The integration of the differential equation system is discussed in Sec. 4. Conclusions are drawn in Sec. 5.

2. SEMIANALYTICAL SOLUTIONS

The starting point is the $D = 1$ Schrödinger equation, which reads

$$\left[-\frac{d^2}{dx^2} + \lambda|x| + icx \right] \Psi_n(x) = E_n \Psi_n(x). \quad (2)$$

This Hamiltonian is obviously PT symmetric, which is known to be a necessary but not sufficient condition for the eigenvalues E_n to be real. On the right half plane, $x \geq 0$, we have to solve

$$\left[-\frac{d^2}{dx^2} + (\lambda + ic)x \right] \Psi_n^+(x) = E_n \Psi_n^+(x). \quad (3)$$

Similarly, for the left half plane, $x \leq 0$, it reads

$$\left[-\frac{d^2}{dx^2} - \lambda x + icx \right] \Psi_n^-(x) = E_n \Psi_n^-(x). \quad (4)$$

By the trivial change of variables

$$t = -x, \quad (5)$$

we are left on the left half plane with

$$\left[-\frac{d^2}{dt^2} + (\lambda - ic)t \right] \Psi_n^-(t) = E_n \Psi_n^-(t). \quad (6)$$

Equations (3) and (6) differ only through the coupling constants of the potential, which are complex conjugate. Consequently, they both have the same formal solutions on their respective domain.

Let us consider the positive x half line. By making the following changes

$$g = \lambda + ic ; z = g^{1/3} \left(x - \frac{E_n}{g} \right), \quad (7)$$

Eq. (3) is transformed into the well known Airy function differential equation [22]

$$\left[\frac{d^2}{dz^2} - z \right] \Psi_n^+(z) = 0. \quad (8)$$

Because we are looking for square integrable solutions, we retain

$$\Psi_n^+(z) \propto Ai(z). \quad (9)$$

The second linear independent solution, $Bi(z)$, is divergent as $\Re z \rightarrow \infty$, and is thus eliminated.

From the above argument, and the analytic properties of the Airy functions, we have

$$\Psi_n^-(z) = \overline{\Psi_n^+(z)} \quad \text{and} \quad \Psi_n(z) = \Psi_n^-(z) \cup \Psi_n^+(z); \quad z = z(x, E_n). \quad (10)$$

The solutions, and in particular the eigenvalues, are fixed by the continuity condition at $x = 0$. Actually, if we write

$$\Psi_n(x) = U_n(x) + iV_n(x), \quad (11)$$

the boundary conditions are given by (up to a normalization factor)

$$U_n(0) = 1 \quad U_n'(0) = 0 \quad V_n(0) = 0 \quad V_n'(0) \neq 0 \quad n \text{ even} \quad (12)$$

and

$$U_n(0) = 0 \quad U_n'(0) \neq 0 \quad V_n(0) = 1 \quad V_n'(0) = 0 \quad n \text{ odd}. \quad (13)$$

Here, U' and V' denote the derivatives with respect to x .

With these boundary conditions, Eq. (8) is solved for $x \geq 0$. The full solutions are then obtained by adding the symmetric or antisymmetric partners for $x \leq 0$.

Handling the Airy functions of complex argument is not so obvious [23, 24]. The procedure to find solutions deserves few explanations. Let us write

$$z = \pm \frac{1}{(1+c^2)^{1/3}} [(x-E)^2 + c^2 x^2]^{1/2} e^{i\theta}; \quad E \geq 0 \quad (14)$$

with

$$\theta(x) = -\frac{2}{3} \arctan c + \arctan \frac{cx}{x-E}. \quad (15)$$

Consider the squared modulus

$$M2(x, E) = \overline{Ai[z(x, E)]} Ai[z(x, E)]. \quad (16)$$

For E fixed, it is a continuous function of x . It shows a monotonic decrease for $x > E$ and an oscillatory pattern for $x < E$, provided the sign of z is chosen positive if $x > E$ and negative if $x < E$. The “sign” of z simply remembers that expressing a complex number through its modulus and phase generates a sign ambiguity. In Fig. 1, the modulus $M2(x, E)$ is displayed for two values of c and two values of E . Note

that otherwise, if the sign of z is kept fixed for all values of x , a discontinuity appears at $x = E$, which has to be rejected.

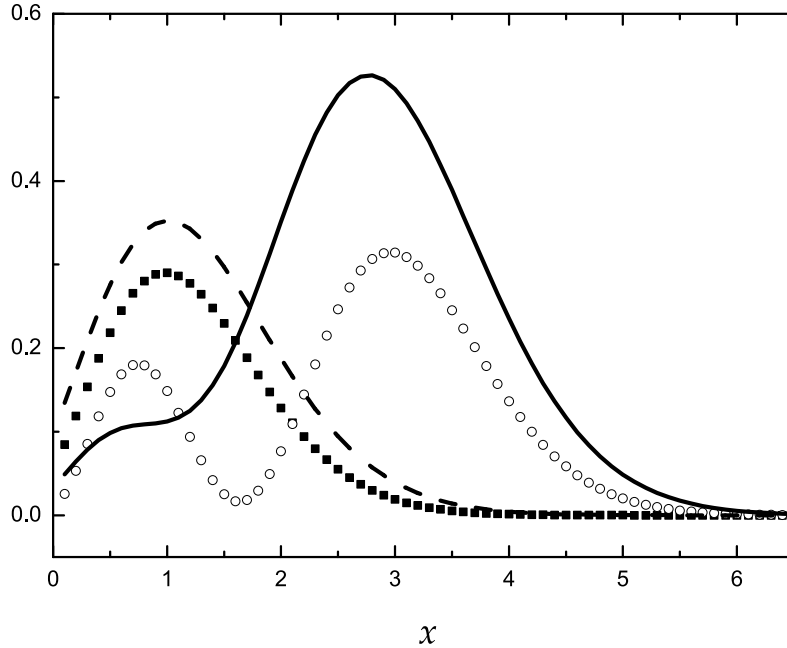


Fig. 1 – Squared moduli of the Airy function for two values of c and two values of E . $c = 0.5$: full squares $E = 2.0$, empty circles $E = 4.0$; $c = 1.0$: dashed line $E = 2.0$, solid line $E = 4.0$.

It has also to be stressed that if c and/or E get large, the oscillatory behavior, typical of the Airy function for negative x , is disappearing. This is shown by the case $c = 1.0$, $E = 4.0$ in Fig. 1.

The search for solutions follows a way similar to the one used for $c = 0$. Namely, the eigenvalues are fixed by setting $x = 0$ at the extrema of the real or imaginary parts on the negative x axis. However, the procedure undergoes an important modification, due to the fact that the solution has to satisfy two conditions.

Let us be more explicit and look at the case of the even states. The boundary conditions imply the real part to be maximum at $x = 0$, where the imaginary part has to be zero. The two conditions are not automatically fulfilled simultaneously. This can be illustrated by the following simple example. Consider

$$f[z(x, E)] = \sin(a + ib) = \sin(a) \cosh(b) + i \cos(a) \sinh(b), \quad (17)$$

where

$$a = a(x, E) ; \quad b = b(x, E).$$

The value of E being fixed, the zeros of the imaginary part are given by the

zeros of $\cos a$. However, they do not coincide with the maxima of the real part, unless the derivative $b'(x) = 0$ at $x = 0$ for $b(0) \neq 0$.

The way to solve the problem, is to remark that the solutions of Eq. (8) are determined up to a constant arbitrary phase. Usually, this phase is irrelevant. Here, however, this degree of freedom can be used to match the continuity conditions at $x = 0$.

In the present case, working on the right half plane, we introduce

$$\Psi_+(z) \rightarrow \Psi_+(z)e^{i\theta_0} = Ai(z)e^{i\theta_0} . \quad (18)$$

For the even states, the conditions to be satisfied read

$$\left. \frac{d}{dx} \left[\Re Ai[x, E] \cos \theta_0 - \Im Ai[z(x, E)] \sin \theta_0 \right] \right|_{x=0} = 0 , \quad (19)$$

and

$$\left[\Re Ai[z(x, E)] \sin \theta_0 + \Im Ai[z(x, E)] \cos \theta_0 \right] \Big|_{x=0} = 0 . \quad (20)$$

The eigenvalues E_n are obtained numerically by solving this system as a function of E . A similar procedure yields the odd states.

However, the system has not necessarily a solution. In other words, it is not always possible to find a phase θ_0 and a real eigenvalue E_n such as the Eqs. (19) and (20) to be satisfied simultaneously. The absence of a solution signals that the eigenvalues are actually complex, and the PT symmetry is spontaneously broken. The occurrence of such a situation clearly depends on the ratio $|c|/\lambda$ and on the quantum number n . This spontaneous breaking of PT symmetry agrees with the fact that the potential ix has no purely real eigenvalue, as shown by Bender and Boettcher [1].

Unfortunately, because we rely on numerical solutions, it is not possible to fix the limits between the real and complex spectrum without tedious numerical works. For this reason, here we shall merely discuss this aspect on the basis of selected examples.

For the sake of illustration, a few eigenvalues have been calculated. For the fixed value $\lambda = 1$, we choose $c = 0.1$, $c = 0.5$, and $c = 1.0$ as typical examples. The results are displayed in Table 1 and compared to the $c = 0$ case. For $c = 0.5$ and $c = 1.0$, the occurrence of complex eigenvalues starts at $n = 3$ and $n = 1$, respectively. In each of these last cases, two complex eigenvalues have been determined above the last real one.

Note that the results do not depend on the sign of c . They are actually complex conjugate of each other. Consequently, we just quote the results for positive c values.

While computing the squared modulus $M2(x, E)$, we found that as c increases, the oscillatory part disappears, and the whole function takes a Gaussian like shape. It

suggests that for the ground state a real eigenvalue exists for large c . For this reason, the ground state eigenvalue has been searched up to $c = 200$. They are indeed real.

Table 1

Real eigenvalues of the linear PT-symmetric potential. The eigenvalues do not depend on the sign of c .

n	$c = 0.0$	$c = 0.1$	$c = 0.5$	$c = 1.0$
0	1.01879	1.02445	1.15245	1.48768
1	2.33811	2.35631	2.8320	$3.8545 \pm i 0.300$
2	3.24829	3.266	3.5274	$5.2996 \pm i 0.234$
3	4.08795	4.1202	$4.8147 \pm i 0.240$	
4	4.82009	4.84587	$5.6683 \pm i 0.214$	
5	5.52056	5.5653		
6	6.16331	6.1947		
7	6.78671	6.844		
8	7.37218	7.407		
9	7.94413	8.014		
10	8.48849	8.5234		

The evolution of $E_0(c)$ is displayed in Fig. 2. It is well fitted by a logarithmic function on the considered c interval:

$$E_0(c) = 1.01879 + (136.2 \pm 5.8) \log [1 + (0.00643 \pm 0.00037)|c|]. \quad (21)$$

On the other hand, $E_0(c)$ also agrees fairly well with a power-law increase of the form

$$E_0(c) \approx -4.0 + 3.35 c^{2/3} ; \quad c \geq 3.0. \quad (22)$$

Comparing again these results with those of Bender and Boettcher [1], we recall that for $\mathcal{V}(x) = (ix)^N$ these authors noticed the following features. For $N \leq 1.42207$, only the ground state has a real energy. This is translated in our work by the disappearance of real eigenvalues for excited states as c is increasing. Furthermore, as N approaches 1 from above, the ground state energy diverges. This last fact incites us to conjecture that adding a small (eventually infinitesimal) $|x|$ component to the potential transforms this divergence into a logarithmic one.

This insight is completed by displaying the ground state wave function for few values of c . The modulus, real, and imaginary parts are displayed in Figs. 3, 4, and 5. We note the strong oscillations of the real and imaginary parts of the ground state wave functions as c increases and gets large.

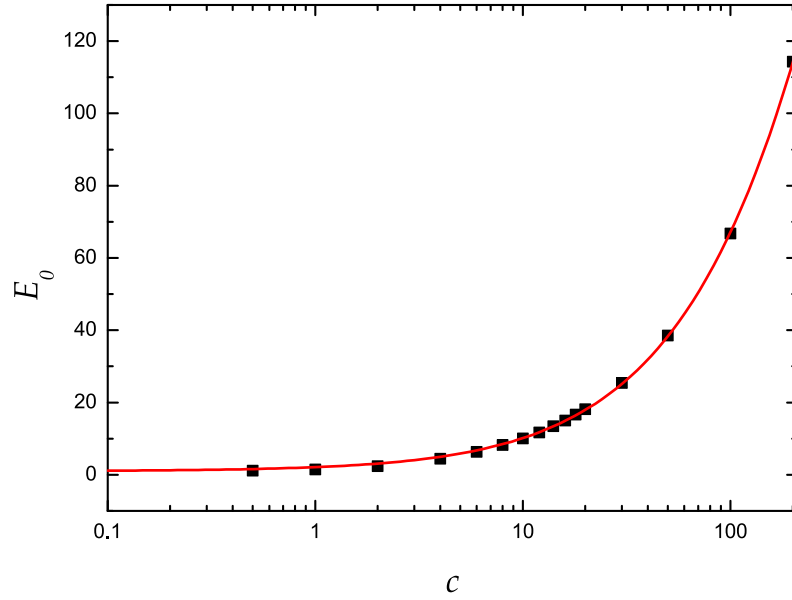


Fig. 2 – Eigenvalues E_0 as function of c . The line gives the fit by Eq. (21).

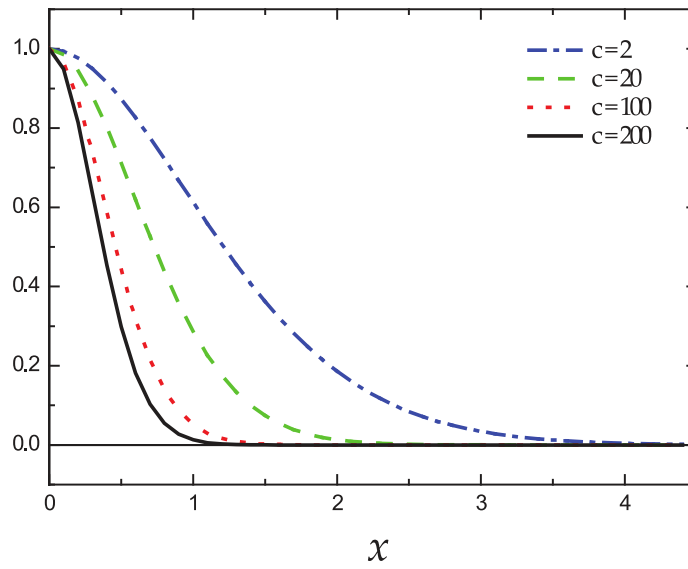


Fig. 3 – Modulus of the ground state wave function for $c = 2, 20, 100,$ and $200,$ respectively. It shrinks as c increases.

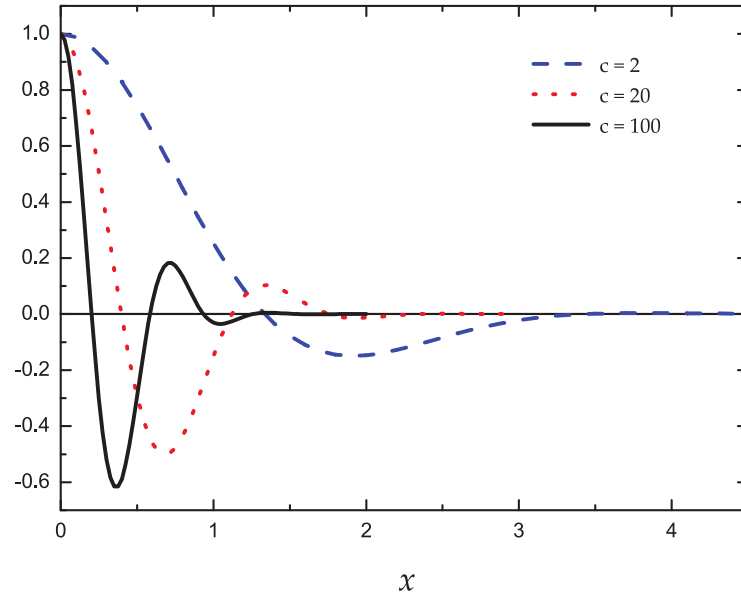


Fig. 4 – Real part of the ground state wave function for $c = 2$ (dashed line), 20 (dotted line), and 100 (solid line), respectively. Note the increasing oscillatory behavior as c increases.

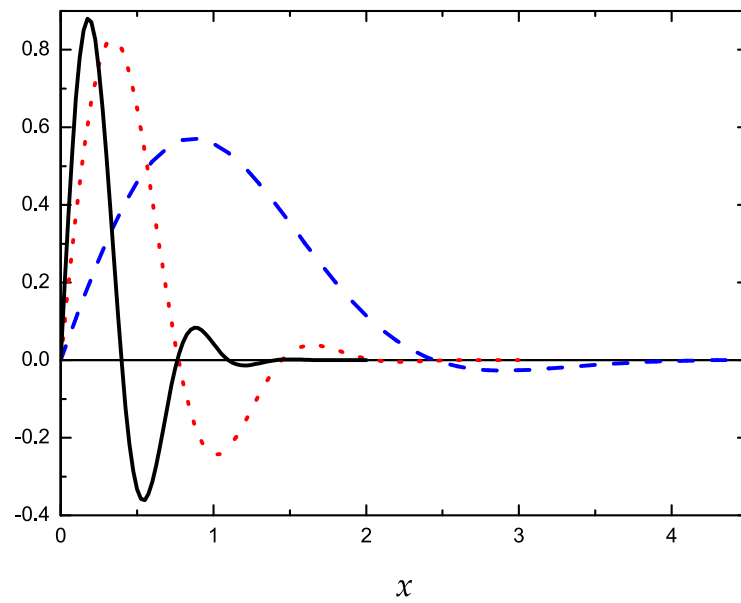


Fig. 5 – The same as in Fig. 4 but for the imaginary part of the wave function.

3. PARAMETRIZING THE AIRY FUNCTION

The usual parametrization of the Airy function is valid either for negative x below $x = -2.0$ or at large x , *i.e.* for $x \geq 2.0$. To get a better understanding of our problem for the ground and first excited states, we have derived an approximation of the Airy function valid around the origin.

The following ansatz

$$A_p(x) = f_0 (x + x_0)^\beta \exp(-\gamma \|x + x_0\|^{3/2}) \quad (23)$$

was found well adapted to the $-2.5 \leq x \leq 2.0$ domain. The precise values of the parameters are not very important, because we work at a qualitative level. Nevertheless, with $\beta = 1.45$,

$$f_0 = 0.848 \pm 0.6\% ; x_0 = 2.39 \pm 0.16\% ; \gamma = 0.568 \pm 0.5\%$$

the approximate function agrees with the actual values to better than 1%, and its maximum arises at $x = -1.0187$ instead of 1.0188.

The extension to the complex plane is obvious :

$$A_p(z) = f_0 (z + z_0)^\beta \exp(-\gamma \|z + z_0\|^{3/2}) . \quad (24)$$

For the ground state, it is sufficient to examine the modulus of the square wave function. If we set

$$Y(z) = (\bar{z} + \bar{z}_0)(z + z_0) , \quad (25)$$

it takes the simple form

$$M2_p(z) = \overline{A_p(z)} A_p(z) = f_0^2 Y(z)^\beta \exp(-2\gamma Y(z)^{3/4}) . \quad (26)$$

To represent the ground state wave function, $M2_p(z)$ must have its maximum at $x = 0$. This leads to the condition

$$Y(0) = \left[\frac{2\beta}{3\gamma} \right]^{3/4} . \quad (27)$$

Note that to simplify the notations, the quantities quoted with (0) are evaluated at $x = 0$.

The second constraint imposes the imaginary part of $A_p(z)$ to be zero at $x = 0$.

Let us parametrize $z + z_0$ with the following expression :

$$z + z_0 = \rho e^{i\theta} + a + ib , \quad (28)$$

where ρ and θ are given by Eqs. (14) and (15), respectively. In this case we have

$$Y(z) = \rho^2 \pm 2\rho(a \cos \theta + b \sin \theta) + a^2 + b^2 . \quad (29)$$

The zero of the imaginary part at $x = 0$ leads to

$$b = \rho \sin \theta . \quad (30)$$

Thus, we get

$$Y(0) = (\pm\rho(0)\cos\theta_0 + a)^2 = \left[\frac{2\beta}{3\gamma}\right]^{3/4}. \quad (31)$$

We have further

$$\rho(0) = (1 + c^2)^{-1/3} E_0 ; \quad \theta_0 = -\frac{2}{3} \arctan c. \quad (32)$$

Consequently, the ground state eigenvalue is given by

$$E_0 = \frac{(1 + c^2)^{1/3}}{\cos\theta_0} \left[a - \left(\frac{2\beta}{3\gamma}\right)^{2/3} \right]. \quad (33)$$

With the parameter values quoted above, this approximation overestimates the ground state eigenvalue at $c = 0$ by 30%. It shows the limitations of the present expression for $A_p(z)$. However, asymptotically, we get

$$E_0 \approx 2.74(1 + c^2)^{1/3} ; \quad c \rightarrow \infty, \quad (34)$$

in reasonable agreement with the fit (22).

This result does not depend sensibly on the parameters of $A_p(z)$. At a qualitative level, it strengthens our conjecture that the ground state energy is real for any c provided $\lambda \neq 0$.

The situation is somewhat more complicated for the first excited state. The same parametrization can be used, but the fact that the conditions imposed to the wave function inverses the role of the real and imaginary parts, changes the problem. The square modulus cannot be used and the constraint has to be applied to the wave function.

Let us write

$$(z + z_0) = \sqrt{Y(z)} e^{i\phi} ; \quad \phi = \arctan \frac{-\rho \sin\theta + b}{-\rho \cos\theta + a}. \quad (35)$$

The condition for the imaginary part to have its maximum at $x = 0$ lead to

$$Y'(0) \left(\frac{\beta}{2} - \frac{3}{4} \gamma Y^{3/4}(0) \right) + \beta \phi'(0) Y(0) = 0. \quad (36)$$

Here, the prime denotes the derivative with respect to x . The derivative of the phase ϕ can be written

$$\phi'(z) = \frac{\chi(z)}{Y(z)} ; \quad \chi(z) = \rho^2 \theta' + \rho' (-a \sin\theta + b \cos\theta) - \rho \theta' (a \cos\theta + b \sin\theta). \quad (37)$$

For the real part to be zero at $x = 0$, we must have

$$a = \rho \cos\theta. \quad (38)$$

By recalling the following quantities at $x = 0$

$$\begin{aligned} \rho(0) &= (1 + c^2)^{-1/3} E_1; \quad \rho'(0) = \rho(0)\theta'(0) = -(1 + c^2)^{-1/3}; \\ Y(0) &= (-\rho(0) \sin \theta_0 + b)^2 \end{aligned} \quad (39)$$

together with

$$\chi(0) = \rho^2(0)\theta'(0) \sin^2 \theta_0 - b\theta'(0)\rho(0) \sin \theta_0 + \rho'(0) \cos \theta_0 (-\rho(0) \sin \theta_0 + b), \quad (40)$$

Eq. (36) becomes an equation for $t = \rho(0) \sin \theta_0$. It has no straightforward analytical solutions, but numerical techniques can be used to reach a desired accuracy.

Actually the important point is that this equation has real solutions only below a critical value of c_1 . Thus the first excited state eigenvalue becomes complex if $c > c_1$. With the parameter values quoted above, we found $c_1 = 0.858$, which is consistent with the values listed in Table 1.

Thus, this simple parametrization of the Airy function yields a good illustration of our findings for the ground and first excited states.

4. INTEGRATING THE DIFFERENTIAL EQUATIONS

Besides the use of the Airy function, we have investigated the numerical integration of the coupled differential equations. This can be achieved in two different ways. First, if we set

$$\Psi_n(x) = R_n(x)e^{i\phi_n(x)}, \quad (41)$$

the system to be solved is given by

$$-R_n''(x) + [g^2(x) + \lambda|x|] R_n(x) = E_n R_n(x) \quad (42)$$

and

$$g_n' R_n + 2g_n R_n' = \pm cx R_n. \quad (43)$$

Here, we have set

$$g_n(x) = \phi_n'(x). \quad (44)$$

The solutions do not depend on the phase $\phi_n(x)$ but on its derivative.

At first glance, it sounds interesting since Eq. (42) looks like an ordinary Schrödinger equation, and Eq. (43) is a first order differential equation. However, $R_n(x)$ is a positive definite function. The usual method, based on counting the zeros of the wave function, cannot be applied here. This difficulty introduces instabilities in determining $g_n(x)$. Thus, apart from the ground state, this approach is not convenient.

Its virtue, however, is to yield the following inequality:

$$E_n(\pm c) \geq E_n(c = 0). \quad (45)$$

It is a strict bound, because the $g^2(x)$ term is acting as a repulsive component of the potential. Note that this bound exists for any complex-valued potential. In its general form, if

$$E_n(\lambda) = \epsilon_n(\lambda) + i\eta_n(\lambda) \quad (46)$$

it can be easily verified that

$$\epsilon_n(\lambda) \geq E_n(0) . \quad (47)$$

Setting $\Psi_n(x) = U_n(x) + i V_n(x)$, the system to be solved is

$$\begin{aligned} -U_n''(x) + \lambda|x|U_n(x) \mp icV_n(x) &= E_nU_n(x) \\ -V_n''(x) + \lambda|x|V_n(x) \pm icU_n(x) &= E_nV_n(x) . \end{aligned} \quad (48)$$

The integration is performed on the right half plane $x \geq 0$, the solutions for $x \leq 0$ being the symmetric or anti-symmetric partners of the positive x ones. The boundary conditions are given by Eqs. (12) and (13) at $x = 0$. At large distances, the modulus of the wave function $\sqrt{U^2(x) + V^2(x)}$ must tend to zero to satisfy the integrability condition.

By choosing E_n and the value of the nonzero derivative at the origin, the system is integrated *via* a Runge-Kutta procedure. As mentioned above, the usual criterion used for the Schrödinger equation cannot be applied here to select the proper solution. Both the real and imaginary parts have an oscillatory behavior. Their zeros are of no help in this case. Therefore, the solution is selected *via* the wave function modulus: it must tangentially approach zero at large distances. As it is well known, applying this criterion is a very difficult task. This difficulty was noticed already more than fifty years ago, in the earlier description of nuclear systems by the density functional method [25, 26].

In practice, solutions are considered up to the point where they reach a minimum close to zero. The one with the lowest minimum value is selected as the solution. It clearly means that in this way the eigenvalues and the wave functions are obtained with a limited accuracy.

For the sake of comparison with the results obtained by using the Airy functions, the system (48) has been integrated for $\lambda = 1$ and $c = 0.5$. The eigenvalues for $n = 0, 1$, and 2 agree with the ones listed in Table 1 within 1%. The selected solutions have their minimum reaching $10^{-5} - 10^{-6}$ of the modulus value at the origin.

It is interesting to compare the wave functions. The results for the ground state are displayed in Figs. 6-8. In Fig. 6 the square of the modulus is plotted, whereas in Fig. 7 and Fig. 8, the real and the imaginary parts of the wave function are given, respectively. At first glance, the agreement between the two estimates is quite satisfactory, showing the coherence of the used numerical approaches. It also gives us confidence in the present method. The only difference perceivable to the eye concerns the tails of the imaginary parts. Confronting the numbers, the agreement

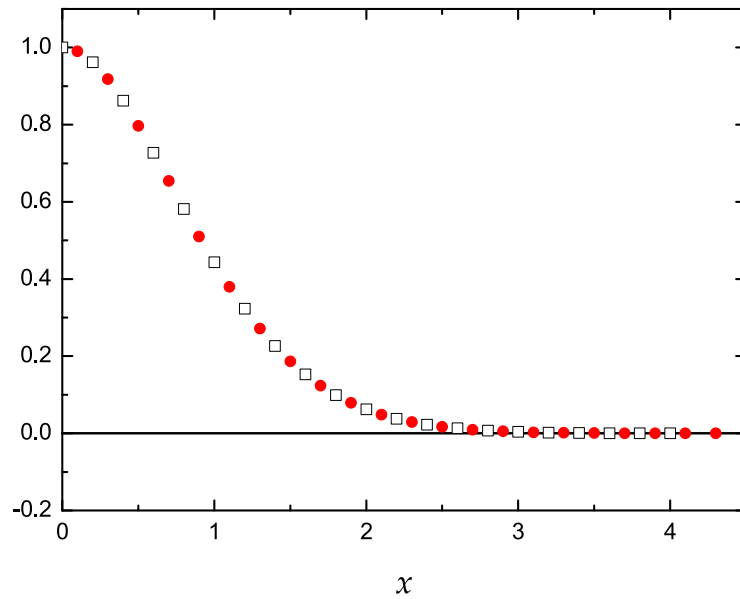


Fig. 6 – Comparison of the modulus of the ground state wave function obtained *via* the Airy function (empty squares) and the direct numerical integration (full circles).

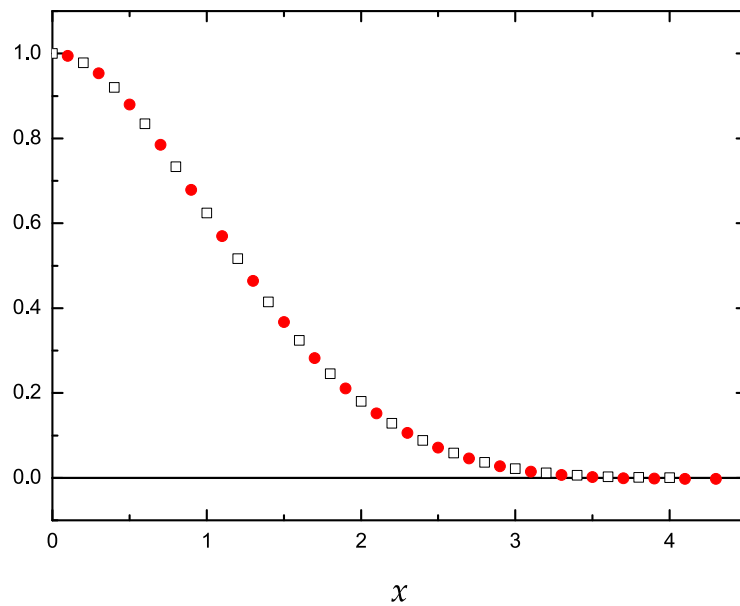


Fig. 7 – The same as in Fig. 6 but for the real part of the ground state wave function.

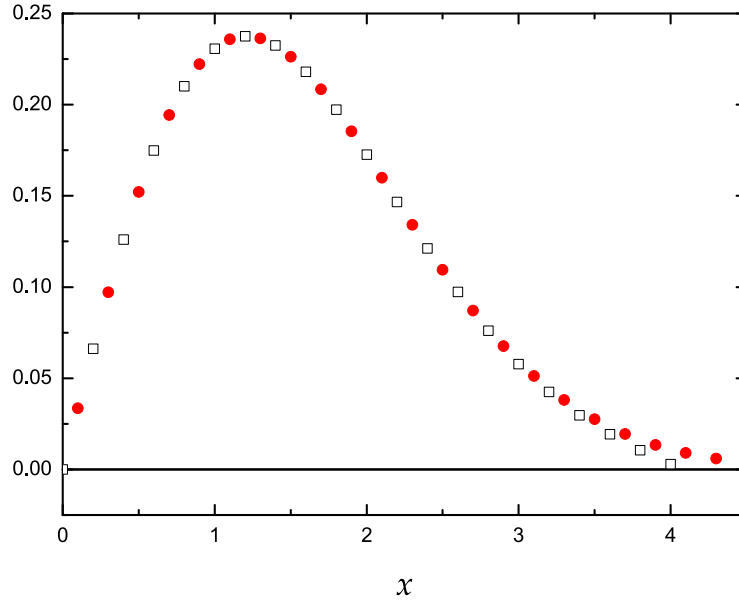


Fig. 8 – The same as in Fig. 6 but for the imaginary part of the ground state wave function.

is better than 0.1% near the origin. It is still of the order of 1% around $x = 2.5$. The disagreement gets large in the tails. It may reach a factor 2 in places where the modulus of the wave functions gets lower than 0.1% of its value at origin.

Caveat: The fact that the eigenvalue becomes complex is more difficult to test with the integration of the differential equation system. Actually the basic criterion of an absolute minimum value of the modulus as it approaches zero is not met. Numerous approximate solutions are found even below the critical limit given by the inequality (22).

5. CONCLUSIONS

We have studied the spectrum of the PT-symmetric complex-valued linear potential $\mathcal{V}(x) = \lambda|x| + icx$. Two methods have been applied. First, use is made of the fact that on each half plane the solution of the Schrödinger equation is the complex Airy function $Ai(z)$. The eigenvalues are found by imposing the continuity conditions at $x = 0$. They are determined numerically. According to the value of $|c|/\lambda$, part of the spectrum has real eigenvalues E_n , in accordance with the PT symmetry of the Hamiltonian. However, as c or n increases the eigenvalues become complex, showing spontaneous breaking of the symmetry.

Special attention has been paid to the ground state, which is somewhat less tedious to investigate numerically than excited states. Solutions were found up to

$c = 200$. The eigenvalues are real. The conjecture that the ground state has indeed a real eigenvalue up to very large c is comforted by the following observation. The oscillations of the squared modulus of the Airy function on the negative x axis vanish as c increases. This behavior indicates a limitation in the number of excited states with real eigenvalues. On the other hand, at large c , the overall shape looks Gaussian. It is an indication that a ground state solution should exist whatever the value of c .

More confidence in the conjecture is obtained by a parametrization of the Airy function on an interval around the origin. By taking into account the necessary conditions required by the wave functions of the ground and first excited states, it clearly shows the ground state energy to keep real for any value of c . On the contrary, the first excited state eigenvalue becomes complex beyond a critical value c_1 .

The second method consists in the numerical integration of the differential equation system for the real and the imaginary parts of the wave function. It is found to work quite well for the ground state. Its results are reasonably close to the ones obtained with the Airy function. The question of the excited states is more delicate. The arising of complex eigenvalues is marked by the absence of a clear criterion to fix a real eigenvalue. Acceptable solutions are found which violate the absolute bound (27).

Acknowledgements. We express our thanks to A. Comtet, J. Mares, and M. Znojil for valuable comments. Thanks are due also to V. Lafage for numerous discussions concerning the numerical methods. Finally R. Mezhoud expresses his thanks for the hospitality extended to him by the IPN Orsay. Finally, we thank Valentin Balanica for his precious help in preparing our files according to the journal's requirements.

REFERENCES

1. C. M. Bender and S. Boettcher, Phys. Rev. Lett. **80** (1998) 5243.
2. A. Mostafazadeh, J. Math. Phys. **43** (2002) 205.
3. M. Znojil, Phys. Lett. A **259** (1999) 220.
4. F. Cannata, G. Junker, and J. Trost, Phys. Lett. A **246** (1998) 219.
5. M. Znojil, Phys. Lett. A **264** (1999) 108.
6. M. Znojil and G. Lévai, Phys. Lett. A **271** (2000) 327.
7. A. Khare and B. P. Mandal, Phys. Lett. A **272** (2000) 53.
8. M. Znojil and M. Tater, J. Phys. A: Gen **34** (2001) 1793.
9. Z. Ahmed, Phys. Lett. A **282** (2001) 343.
10. B. Roy and R. Roychoudhury, J. Phys. A Math. Theor. **40** (2007) 8479.
11. C. M. Bender, D. C. Brody, and H. F. Jones, Phys. Rev. Lett. **89** (2002) 270401; Phys. Rev. Lett. **92** (2004) 119902.
12. A. Ruschhaupt, F. Delgado, and J. G. Muga, J. Phys. A: Math. Gen. **38** (2005) L171.
13. B. Liu, L. Li, and D. Mihalache, Rom. Rep. Phys. **67** (2015) 802.
14. D. Mihalache, Rom. Rep. Phys. **67** (2015) 1383.
15. M. Wimmer, M.-A. Miri, D. Christodoulides, and U. Peschel, Sci. Rep. **5** (2015) 17760.

16. P. Li, B. Liu, L. Li, and D. Mihalache, *Rom. J. Phys.* **61** (2016) 577.
17. Yi-Xiang Chen, *Nonl. Dyn.* **85** (2016) 2801.
18. C. M. Bender, *Rep. Prog. Phys.* **70** (2007) 947.
19. Y. He, X. Zhu, and D. Mihalache, *Rom. J. Phys.* **61** (2016) 595.
20. V. V. Konotop, J. Yang, and D. A. Zezyulin, *Rev. Mod. Phys.* **88** (2016) 035002.
21. C. M. Bender, F. Cooper, P. N. Meisinger, and Van M. Savage, *Phys. Lett. A* **259** (1999) 224.
22. See, for instance, S. Flügge, *Practical Quantum Mechanics*, Springer Verlag, 2nd edn., 1994; M. Abramovitz and I. A. Stegun *Handbook of Mathematical Functions* National Bureau of Standards, 10th edn., Washington, 1972.
23. A. Comtet, J.-M. Luck, C. Texier, and Y. Tourigny, *J. Stat. Phys.* **150** (2013) 13.
24. O. Vallée and M. Soares, *Airy functions and applications to physics*, Imperial College Press, London, 2010.
25. K. Kumar, K. J. Le Couteur, and M. K. Roy, *Nucl. Phys.* **42** (1963) 524.
26. K. A. Brueckner, J. R. Buchler, S. Jorna, and R. J. Lombard, *Phys. Rev.* **171** (1968) 1188.